Heterotrophic soil respiration and carbon cycling in geochemically distinct African tropical forest soils

Benjamin Bukombe[1], Peter Fiener[1], Alison M. Hoyt[2], Laurent K. Kidinda[3], Sebastian Doetterl[4,1]

[1]Institute of Geography, Augsburg University, Augsburg, 86159, Germany
[2]Max Planck Institute for Biogeochemistry, Jena, 07745, Germany
[3] Institute of Soil Science and Site Ecology, Technische Universtität Dresden, Tharandt, 01737, Germany
[4] Department of Environmental System Science, ETH Zurich, Zurich, 8092, Switzerland

Correspondence to: *S. Doetterl (sdoetterl@usys.ethz.ch)*

Abstract

Heterotrophic soil respiration is an important component of the global terrestrial carbon (C) cycle, driven by environmental factors acting from local to continental scales. For tropical Africa, these factors and their interactions remain largely unknown. Here, using samples collected along topographic and geochemical gradients in the East African Rift Valley, we study how soil chemistry and fertility drive soil respiration of soils developed from different parent materials even after many millennia of weathering. To address the drivers of soil respiration, we incubated soils from three regions with contrasting geochemistry (mafic, felsic, and mixed sediment) sampled along slope gradients. For three soil depths we measured the potential maximum heterotrophic respiration under stable environmental conditions as well as the radiocarbon content ($\Delta^{14}C$) of the bulk soil and respired CO_2. Our study shows that soil fertility conditions are the main determinant of C stability in tropical forest soils. We found that soil microorganisms were able to mineralize soil C from a variety of sources and C quality under laboratory conditions representative of tropical topsoil. However, in the presence of organic carbon sources of poor quality or the presence of strong mineral related C stabilization, microorganisms tend to discriminate against these energy sources in favor of more accessible forms of soil organic matter, resulting in a slower rate of C cycling. Furthermore, despite similarities in terms of climate and vegetation, soil respiration showed distinct patterns with soil depth and parent material geochemistry. The topographic origin of our samples was not a main determinant of the observed respiration rates and $\Delta^{14}C$. In situ, however, soil hydrological conditions likely influence soil C stability by inhibiting decomposition in valley subsoils. Our results demonstrate that even in deeply weathered tropical soils, parent material has a long-lasting effect on soil chemistry that can influence and control microbial activity, the size of subsoil C stocks, and the turnover of C in soil. Soil parent material and its control on soil chemistry need to be taken into account to understand and predict C stabilization and rates of C cycling in tropical forest soils.

1. Introduction

Tropical forests and the soils therein are one of the most important and largest global terrestrial carbon (C) pools and serve as important climate regulators (Cleveland et al., 2011; Kearsley et al., 2013; Lewis et al., 2009; Sayer et al., 2011). They contain about one third (421 Pg C) of the global soil organic carbon stock (SOC) in the upper one meter of soil (Köchy et al., 2015) and are characterized by high annual C turnover rates (Raich and Schlesinger, 1992). Generally, climatic parameters (temperature and precipitation) and vegetation input are regarded as the main factors controlling C dynamics in natural tropical systems (Davidson et al., 2000; Davidson and Janssens, 2006; Rey et al., 2005). Vegetation and climate can stimulate or hamper microbial activity and mineralization of C through quality and quantity of organic matter (OM) input to soil (Fontaine et al., 2007), and the availability of water and energy to drive microbial processes. However, recent studies show that SOC dynamics are controlled by a much more complex interplay of geochemistry, topography, climate and biology (Doetterl et al., 2015b, 2018; Haaf et al., 2021; Luo et al., 2017, 2019) much like pedogenesis in general. For example, on average 72% of SOC in humid forest biomes is stabilized by interaction with the mineral phase in soil organo-mineral interactions and occlusion by aggregation (Kramer and Chadwick, 2018). Geology can control C dynamics as soils developed from felsic parent material (high SiO_2, low Fe & Al, slow chemical weathering rate) provide less potential for C stabilization and a lower capacity to release rock-derived nutrients than soils developed from mafic parent material (low SiO_2, high Fe & Al, fast chemical weathering rate), limiting organic matter input. Additionally, topography through its control on water and soil fluxes may influence C dynamics by altering C respiration and input along slope gradients (Berhe et al., 2008). Hydrological features related to topography in tropical forests are likely to influence C cycling and explain spatial patterns of SOC distribution locally by limiting C decomposition in water saturated valleys (Kwon et al., 2013). Finally, some soils developed from sedimentary parent material can contain a large fraction of fossil organic carbon (f_{FOC}) of generally poorer quality than fresh organic matter inputs, which can be resistant to decomposition under in situ environmental conditions (Kalks et al., 2021). Hence, in order to explain SOC and its exchange between soil and the atmosphere, the interactions of geochemical, geomorphic and climatic drivers are central (Angst et al., 2018; Berhe et al., 2012; Doetterl et al., 2015b; von Fromm et al., 2021; Kramer and Chadwick, 2018; Luo et al., 2017)

To date, it is not clear if the relationships between soil geochemistry, topography and climate identified for temperate ecosystems also apply in the tropics. Especially for the African tropics, more work is required to understand how soil geochemical, physical, biological and topographic features interact to influence SOC dynamics. Established observatories in African tropical forests have focused mostly on biodiversity preservation and C storage in the phytosphere (Tyukavina et al., 2013; Xu et al., 2017), while soils have received much less attention and remain understudied. Generally, data on SOC dynamics from tropical regions are rare compared to the temperate zone, originating mostly from the Amazon basin (Quesada et al., 2020; Schimel et al., 2015; Schimel and Braswell, 2005) and their application to the African tropics may be limited. For example, atmospheric nitrogen deposition is much higher in sub-Saharan Africa than in other tropical regions due to large

amounts of recurring biomass burning originating from savanna and dry forests north and south of the humid tropics (Bauters et al., 2018).

Furthermore, long-term chemical weathering in tropical systems has led to the depletion of rock-derived nutrients in soils and has limited the capacity of microorganisms and plants to access these nutrients (Liu et al., 2015; Vitousek and Chadwick, 2013). It is likely that variation in soil weathering stage and nutrient availability in tropical forests affect soil C storage and the exchange of C between plants, soil and the atmosphere. For example, due to their tight coupling driven by the metabolic needs of plants and microorganisms, changes in nutrient availability such as nitrogen (N) and phosphorus (P) can greatly alter the terrestrial C cycle, partly because CO_2 uptake by terrestrial ecosystems strongly depends on N and P availability (Fernández-Martínez et al., 2014). Furthermore, low N and P availability limits microbial growth and activities and therefore affects the cycling of organic matter (Jing et al., 2020; Liu et al., 2015). Thus, nutrient limitations in highly weathered tropical soil likely force plant communities to alter belowground and aboveground C allocation (Doetterl et al., 2015a; Fisher et al., 2013; Wright et al., 2011), with more roots growing in organic rich topsoil, reducing C input to deeper soil layers (Addo-Danso et al., 2018), thereby affecting SOC stocks.

Additionally, along soil age gradients, SOC stabilization by clay first increases and then decreases, with a reduction in reactive mineral surfaces as weathering advances (Doetterl et al., 2018; Kramer and Chadwick, 2018). As a consequence, clay in old tropical soils has a rather limited potential to protect C against microbial decomposers compared to younger temperate soils (Doetterl et al., 2018; Ngongo et al., 2009). In contrast, stable microaggregates rich in iron (Fe) and aluminum (Al) oxyhydroxides found in abundance in tropical soils (Bruun et al., 2010; Torres-Sallan et al., 2017) seem to be of greater importance in stabilizing C in tropical soils, as concentrations of Al and Fe are commonly higher than in many temperate soils (Khomo et al., 2017). This is confirmed by studies conducted across a wide range of tropical ecoregions showing that SOC is mainly regulated by Fe or Al (hydr) oxides, more so than by clay content (Fang et al., 2019; von Fromm et al., 2021; Rasmussen et al., 2018).

Hence, understanding tropical soils C dynamics ultimately depends on our mechanistic understanding of these complex interactions and the ability to determine the primary environmental controls on SOC content and respiration. In our study, we aim to answer if C release through heterotrophic respiration from forest soils in the humid tropics follows predictable patterns related to geochemical soil properties and topography. We postulate that, in the absence of anthropogenic disturbance, soil geochemistry derived from its parent material has a lasting effect on soil C respiration due to its influence on stabilization mechanisms and soil fertility, even in deeply weathered natural tropical soils. We selected soils in our study that developed from geochemically distinct parent material along slope gradients under comparable tropical climate and vegetation. We hypothesize that (1) specific soil respiration and the $\Delta^{14}C$ signature of potential soil respiration in tropical soils are primarily controlled by geochemical properties related to soil fertility derived from and varying with soil parent material. These

variations in soil fertility can stimulate or inhibit microbial activity and increase or decrease soil C decomposition rates. (2) The presence or absence of C stabilization mechanisms, in soils, related to mineral geochemistry and soil formation, can increase SOC stocks and decrease heterotrophic C respiration rates by creating an energetic barrier for C decomposers, for example through complexation with organic molecules or by forming stable (micro) aggregates. (3) The topographic origin of a soil sample controls specific soil respiration and its $\Delta^{14}C$ signature indirectly through the environmental conditions under which soil C decomposition took place in situ, modifying the quality and quantity of the available SOC stock prior to the experiment.

Materials and Methods

2.1. Study sites

Our study sites are located in three forested national parks along the Albertine Rift System at the borders between Uganda, Rwanda and the Democratic Republic of the Congo (DRC), in the East African Rift Valley system (Doetterl et al., 2021). The climate of the study region is classified as tropical humid with weak monsoonal dynamics (Köppen Af-Am). Mean annual temperature (MAT) is around 15.3-19.3 °C and mean annual precipitation (MAP) varies between 1697-1924 mm (Fick and Hijmans, 2017). Study sites are located between 1300-2200 m above sea level in sloping mountainous landscapes with small flat plateaus and ridges, followed by longer, steep slopes (up to 60% slope steepness) and small, v-shaped valleys. The dominant vegetation in all forests across the region is primary tropical mountain forest with smaller differences in biodiversity and species composition (van Breugel et al., 2020; Doetterl et al., 2021; Verhegghen et al., 2012)

Across the study region, we investigated soils developed from three geochemically distinct parent materials (mafic magmatic, felsic magmatic and mixed sedimentary rocks). Study sites in the DRC are located in Kahuzi-Biega National Park (-2.31439° S; 28.75246° E) where soils have developed from mafic magmatic rocks, a result of volcanism in the East African Rift System (Schlüter, 2006). Mafic magmatic rocks in the region are characterized by high Fe and Al and low Si content as well as a high content of rock-derived nutrients such as base cations, and P (Table 1). Study sites in Uganda are located in Kibale National Park (0.46225° N; 30.37403° E) where soils have developed from felsic magmatic and metamorphic rocks. The felsic magmatic rocks in our study region are characterized by the gneissic-granulitic complex with low contents of Fe, and Al, and high Si content. Unlike mafic, felsic magmatic rocks in our study sites are characterized by low content of rock-derived nutrients (Table 1). Study sites in Rwanda are located in Nyungwe National Park (-2.463088° S; 29.103834° E) where soils have developed from a mixture of sedimentary rocks of varying geochemistry. These sediments are mostly dominated by quartz-rich sandstones and schist layers spanning along the Congo-Nile divide in the western province of Rwanda (Schlüter, 2006). Similar to the felsic magmatic soils, mixed sediments in our study sites are characterized by low Fe and Al content but high Si content and low content of rock-derived nutrients. A specific feature of the mixed sedimentary rocks in our study

region is the presence of fossil organic carbon (Table 1). Fossil organic carbon in these sediments is further characterized by a high C:N ratio (153.9 ± 68.5), and is depleted in N (Doetterl et al., 2021; Reichenbach et al., 2021)

Dominant soil types in the region are various forms of deeply weathered tropical soils. Following the World Reference Base for Soil Resources (IUSS Working Group WRB, 2015), soils in the mafic region are described as umbric, vetic and geric Ferralsol and ferralic vetic Nitisols. Soils in the mixed sediment region and the felsic region are described as geric and vetic Ferralsol. Soils in valley bottoms can locally show gleyic features, and Ferralsols there are paired with fluvic Gleysols. Soil texture across our sites was generally similar and classified as clay loam with highest clay content in the mafic region (54.20±2.91%), highest silt content in the mixed sediment region (22.63±2.25%). Highest sand content was reported for the felsic region (51.90±1.48%). Bedrock could not be reached in any soils located under forest vegetation (>3 m) confirming the deep weathering of the parent material during soil formation. The weathering front was found in nearby mining and road cuts only at depths >10 m. Hence, the investigated soils and their geochemical properties, created through many millennia of weathering, can be interpreted as the end members of pedogenetic alteration for the upper meter of soil, which is the focus of our study.

Table 1. Chemical composition of unweathered rock samples representing the soil parent material in the investigated three geochemical regions. Values represent mean ± standard errors (N=6, 10 and 3 for mafic, felsic and mixed sediment respectively).

Geochemical region	C[%]	Fe [%]	Al [%]	Si [%]	Ca [%]	K [%]	Mg [%]	P [%]
Mafic	0	8.98 ±0.75	6.26±1.15	14.22±0.82	0.58±0.23	0.08±0.03	1.25±0.13	0.36±0.05
Felic	0	1.08±0.5	0.51±0.38	37.28±1.87	0.01±0.004	0.01±0.006	0.01±0.005	0.005±0.002
Mixed sediment	4.03	2.32±0.99	0.61±0.23	36.11±4.04	0.005±0.005	0.07±0.03	0.01±0.005	0.02±0.009

2.2. Soil sampling

As part of a larger project (Project TropSOC) (Doetterl et al., 2021), soil samples were collected following a catena approach with three 40 m x 40 m plots (field replicates) at four topographic positions (plateau, upper slope, middle slope and valley/foot slope), resulting in 12 plots within each geochemical region (mafic, felsic, and mixed sediment). Each plot was subdivided into four subplots of 20 m x 20 m from which four 1-meter soil cores were taken using a cylindrical soil core sampler for undisturbed sampling. Cores were separated into 10 cm increments. The corresponding increments from four cores per plot were mixed into a depth-explicit composite sample. For the experiments conducted in this study, we selected 112 soil samples covering three depth categories including topsoil (0-10 cm), shallow subsoil (30-40 cm), and deep subsoil (60-70 cm). We selected these three depth intervals as they cover a wide range of biogeochemical properties in soil and various levels of organic matter input to soil, both in terms of quantity (more C input near the surface, less at depth) and quality (leaf litter + root derived

C in topsoil; root-derived C in subsoil). Note that as part of our own data analyses, published values for SOC stocks and bioavailable Phosphorus (bio-P) (Doetterl et al. 2021) are reported in results section 3.1. For a more detailed description of the study design, soil sampling, sample treatment and analysis of all biogeochemical parameters used in this study, see the complete database description in Doetterl et al. (2021).

2.3. Laboratory Experiments

Potential heterotrophic soil respiration

Heterotrophic respiration per gram SOC (specific potential respiration "SPR", $\mu gCO_2\text{-}C\ gSOC^{-1}\ h^{-1}$) was assessed in a lab-based incubation experiment and measured for the three sampling depths across geochemical and topographic gradients. Briefly, 50 g of 12 mm sieved air-dried soil were weighed into a 100 ml beaker. Soil samples were sieved to 12 mm to homogenize the substrate while maintaining aggregate structure at a low level of disturbance. Soil moisture was adjusted to 60% water holding capacity, selected as the optimum water content level for microbial activity (Rey et al., 2005). Each beaker was placed inside an open 955.5±1.3 ml mason jar covered with parafilm, allowing for air exchange to avoid oversaturation of CO_2 within the jar that could inhibit microbial activity. Samples were then incubated at 20 °C, similar to the annual mean temperatures of the study sites. Except for keeping soil moisture steady by adding water when necessary, no further amendments were made to the incubated soils. Following a pre-incubation period of 4 days to allow equilibration, we incubated all samples for 120 days and sampled periodically every 1 to 14 days throughout the experiment with longer intervals towards the end of the experiment as respiration rates leveled off. The incubation experiment ended when additional CO_2 production was not detectable within measurement error. This was the case when the standard deviation of means of the respiration rate between three consecutive measurement time points was smaller than the standard deviation between three replicates of the same measurement time point. For CO_2 accumulation prior to sampling, mason jars were sealed for several hours per measurement point. The accumulated CO_2 was sampled using a syringe and transferred to pre-evacuated 20 ml vials. To avoid CO_2 saturation effects during measurements, potentially influencing microbial decomposition processes, jars were flushed with background air from the laboratory and checked for moisture content, before and after sealing to accumulate CO_2. Generally, CO_2 samples were taken after accumulating between 1000-3000 ppm CO_2. The CO_2 concentration of the extracted gas was subsequently measured using a gas chromatograph (Trace^{TM} 1300, Thermo Fisher Scientific, Massachusetts, United Stated) calibrated with five CO_2 standards covering the range of measured concentrations (0, 500, 1000, 5000, 10000 ppm CO_2). Further, the measured CO_2 was corrected for the CO_2 concentration of the ambient air that was used to flush the jars before closing for CO_2 accumulation. After each measurement was completed, each jar was opened and covered with parafilm to allow gas diffusion between CO_2 accumulation periods. In this way, an average of 12 observations of CO_2 production rate per incubated sample were conducted during the course of the experiment. Our aim was to compare average respiration between samples rather than the absolute values through the entire period of the experiment. Thus, we analysed data as the

weighted average of SPR over the entire length of the experiment after respiration levelled off. We defined the weight by how many days of the incubation experiment each observation represents. Additionally, we incubated 20% of all samples in triplicate to assess the average difference between samples for the experiment. The resulting average standard error of the mean between the three lab replicates was 9.6%.

$\Delta^{14}C$ of bulk soil and respired CO_2

We measured the soil radiocarbon (^{14}C) content of both bulk soil (SOC) and the corresponding respired CO_2 from our incubation samples. Bulk soil $\Delta^{14}C$ provides an indicator of the persistence of C in the soil and its age (Shi et al., 2020), while the $\Delta^{14}C$ of the respired CO_2 reflects more actively cycling C (Trumbore, 2009). The difference between these measures (Δ-$\Delta^{14}C$) can provide an indicator of how homogeneous or heterogeneous the system is (Sierra et al., 2018), depending whether the $\Delta^{14}C$ signature of the respired CO_2 is similar to, or differs from the bulk soil $\Delta^{14}C$. Radiocarbon analyses were conducted on composite samples of the bulk soil replicates used for incubation and correspondingly on composite samples of the respired CO_2 during incubation. Bulk soil $\Delta^{14}C$ was measured on soil samples before the incubation started. The $\Delta^{14}C$ of respired CO_2 was measured from CO_2 that accumulated over the initial period following the pre-incubation period. The CO_2 accumulation period varied depending on sample. For top and shallow subsoil with higher CO_2 respiration rates it took on average 4-7 days while for deep soil with low CO_2 it took 10-15 days to accumulate 1 mg C needed for $\Delta^{14}C$ analysis. After accumulation, 120 ml of headspace gas from each field replicate incubation jar was sampled using a syringe. These replicate samples were transferred into a single 400 ml pre-evacuated Restek canister for composite analysis. Radiocarbon concentrations presented in our study are given as fractions of a modern oxalic acid standard following the conventions of Stuiver and Polach (1977). All measurements were done with the MICADAS Mini Carbon Data System (IonPlus, Switzerland) at the AMS facility at Max Planck Institute for Biogeochemistry (Jena, Germany) (Steinhof et al., 2017).

2.4. Assessing fossil vs. biogenic organic carbon

Radiocarbon measurements were used to assess differences in the age of respired versus soil carbon, and to estimate the potential contribution of fossil organic C to the total soil organic C content and to CO_2 respired during incubations. For the latter, we focused on the mixed sediment region, as this is the only geochemical region in our study where soil parent material contains fossil organic C. We used a two-end member mixing model following (Schuur et al., 2016) to calculate the fraction of the C in the sample originating from biogenic vs. fossil organic C as follows:

$$F_{FOC} * f_{FOC} + F_{bio} * f_{bio} = F_{sample} \quad (1)$$

where F_{FOC}, F_{bio} and F_{sample} represent the fraction modern radiocarbon (F), of fossil organic C, biogenic C and the measured sample (bulk soil organic C or respired CO_2) respectively; and f_{FOC} and f_{bio} represent the proportion of fossil organic C and

biogenic C contributing to a sample's total C content. For this estimate, we assumed that fossil organic C is free of ^{14}C due to the high age of parent material (Doetterl et al., 2021; Schlüter, 2006). Further, we assumed that radiocarbon values of biogenic SOC (F_{bio}) in the mixed sediment region follow the same trend with soil depth as the mean radiocarbon content measured depth-explicit from plateau soils of the mafic and felsic regions (regions without fossil organic C), and that these values represent biogenic SOC from active biological cycling in plant-soils systems (Cerri et al., 1985; Kalks et al., 2021). However, because rates of biogenic C cycling likely vary across sites, with potentially slower biogenic cycling in mixed sediment region (see discussion), this estimate is likely an upper bound on the fossil organic C contribution to these samples. Based on these assumptions, we reduced Eq. (1) and solved for the proportion of biogenic organic C (f_{bio}) as follows:

$$f_{bio} = F_{sample} / F_{bio} \quad (2)$$

The fraction of fossil organic C was then calculated as follows:

$$f_{FOC} = 1 - f_{bio} \quad (3)$$

2.5. Statistical analysis

Assessing patterns of respiration and $\Delta^{14}C$

To examine differences in mean SPR in relation to the three main factors topographic position −soil depth and geochemical region− we conducted three-way analysis of variance (ANOVA). Before ANOVA, we conducted residual analysis to test for the assumptions of ANOVA, Shapiro-Wilk's test of normality distribution and Levene's test for homogeneity of variances (Shapiro and Wilk, 1965). In most cases, the homogeneity and normality tests did not meet the requirement due to the natural variability of the samples and the factorial sampling design. Hence, we used square root and log transformation to approximately conform to normality and conducted the ANOVA tests on the transformed dataset. To compare the means of multiple groups, post-hoc pairwise comparison was applied using Bonferroni correction (Day and Quinn, 1989) or Tamhane T2 in the case of unequal variances (Tamhane, 1979).

Predicting SPR and $\Delta^{14}C$

Multiple linear regression was used to assess the explanatory power of soil properties to predict SPR and the difference between the soil and respired CO_2 $\Delta^{14}C$ signature (Δ-$\Delta^{14}C$). Before running regression models, we extracted a wide range of physico-chemical soil properties and SOC quality indicator (C:N) for our investigated soils, where, in parallel studies, soil C stabilization mechanisms were assessed by Reichenbach et al. (2021) and microbial activity parameters (CNP enzymes and microbial biomass) assessed during our incubation experiment (Table B1) by Kidinda et al. (2020). Overall, our dataset

consisted of 37 independent variables and 112 aggregated observations for each of our target variables (For CO_2: Aggregated from 1350 individual observations of SPR over the course of the experiment). As multicollinearity and autocorrelation between independent variables was to be expected due to this large number of independent variables and a relatively small number of aggregated observations, we conducted rotated principal component analysis (rPCA) for dimension reduction (Jolliffe, 1995), before regression analysis. We then named all retained rotated components (RCs) based on the loadings of the original variables and interpreted them for the likely underlying mechanisms that can affect C dynamics (Table B1). We used a threshold of $r > 0.5$ to decide whether an independent variable that is loaded into an RC is used for the mechanistic interpretation of the RC or not. We used an eigenvalue >1 and explained proportion of variance >5% for each RC as criteria to include or exclude RCs into our regression models (James et al., 2013; Jolliffe, 1995). Furthermore, we used p-Values ($p<0.1$) and standardized coefficients to evaluate the contribution of explanatory power of individual RCs to the overall model while the F-statistic was used to evaluate the overall relationship between RCs and SPR or Δ14C for every model. Note that we found no statistical difference in SPR or $\Delta^{14}C$ between the plateau and slope positions within each studied geochemical region (mafic, felsic, and mixed sediment). Across geochemical regions and soil depths, SPR, and $\Delta^{14}C$ differed only between valleys and non-valley positions. Hence, all further analyses were done after splitting the data into two subsets: (1) non-valley positions (plateau, upper slope, and middle slope) versus (2) valley positions (valleys and foot slope). When predicting our target variables, each regression analysis was done for three subsets of data: One model containing all data, one with only topsoil data and one with only subsoil data. Samples from valley positions were excluded from this part of the analysis due to the sample size of the valley subset being too small (9 sites, 27 soil samples) for reliable regression analyses. Hence, our analysis to identify controls via regression and RCs to predict SPR and $\Delta^{14}C$ is focused on non-valley positions (27 sites, 85 soil samples).

Assessing relative importance of explanatory variables

Lastly, we assessed the relative importance of each individual RC in predicting the target variables by interpreting the standardized coefficients (-1 to 1) and p-values associated with each regression model. When predicting target variables with all data, soil depth was included as an additional explanatory variable beside the rotated components (RCs). We did this in order to avoid interpreting variables as being important for the model when they were instead just auto-correlated with soil depth. In a final step, we used partial correlation analysis following Doetterl et al. (2015b), to interpret the explanatory power of independent variables in our model, while controlling for soil depth. We contextualize our findings with respect to microbial (extracellular enzyme activity) (Kidinda et al., 2020) , mineralogical (pedogenic oxides) (Reichenbach et al., 2021) and soil fertility parameters (available nutrients and exchangeable base cations) (Doetterl et al., 2021). For all statistical tests, due to the relatively small sample size and to avoid Type II statistical errors, a threshold of $p<0.1$ was used to indicate significant difference. R^2 and root mean squared error (RMSE) were used as evaluation metrics for model performance. All statistics were performed using R statistical software and the packages “psych”, and “ppcor” (R Core Team, 2019).

3. Results

3.1 Patterns of respiration and $\Delta^{14}C$

Topography and soil depth

For all three geochemical regions in non-valley topographic positions, SPR and $\Delta^{14}C$ decreased with soil depth (Fig. 1a-b and 2a-b, respectively). For SPR, differences with soil depth were smallest for sites in the mixed sediment and largest for sites in the mafic region. For $\Delta^{14}C$, relative changes with depth were similar for mafic and felsic geochemical regions in both soil and respired CO_2, but samples from the mixed sediment region were consistently more depleted in $\Delta^{14}C$ than their counterparts from mafic and felsic regions (Fig. 2a-b).

In valley positions, SPR did not follow a clear trend with soil depth. In the mafic region, SPR decreased with depth, while in the felsic region it increased with depth (Fig. 1b). No statistically significant differences in SPR with depth were observed for the mixed sediment region (Fig. 1b). All regions show a strong trend of depletion of $\Delta^{14}C$ with depth in valleys (Fig. 2a-b).

Geochemistry and soil depth

Consistently, for non-valley profiles, SPR was higher in felsic and mafic regions than in the mixed sediment region (Fig.1a). Additionally, while topsoil samples between mafic and felsic did not show differences in SPR, subsoil samples in the felsic region showed higher SPR than their mafic counterparts and SPR in the mixed sediment region was generally lowest. The $\Delta^{14}C$ values of both soil and respired CO_2 in mafic and felsic regions were not significantly different from each other for either top- or subsoil. Bulk soil samples from the mixed sediment region were consistently depleted compared to their mafic and felsic counterparts.

At valley positions, SPR in topsoil was not significantly different for mafic and felsic samples. Mixed sediment samples were slightly lower in SPR in topsoil than their mafic and felsic counterparts, but not nearly as low as at non-valley positions (Fig. 1b). In subsoils, SPR was highest in the felsic and lowest in the mafic region, while the mixed sediment region was not significantly different from the mafic samples (Fig. 1b). As in non-valley counterparts, $\Delta^{14}C$ activity in valley positions was lowest in samples from the mixed sediment region and differences between the mafic and felsic regions were generally small (Statistical test was not possible due to small sample size, Fig. 2a-b).

Patterns of SOC stock and available nutrient across geochemical region

SOC stocks in the topsoil were similar across all geochemical regions. However, SOC stock significantly decreased with depth for the felsic but not for the mafic or mixed sediment region (Figure 1c). Available phosphorus (Bio-P) was not significantly different between the mafic and felsic regions except in the topsoil where samples from the mafic region show the highest

values (Figure 1d). Bioavailable-P decreased with soil depth for the mafic and felsic regions, but not for the mixed sediment region where it was consistently lower than in soils of the mafic and felsic regions across all sampled depths.

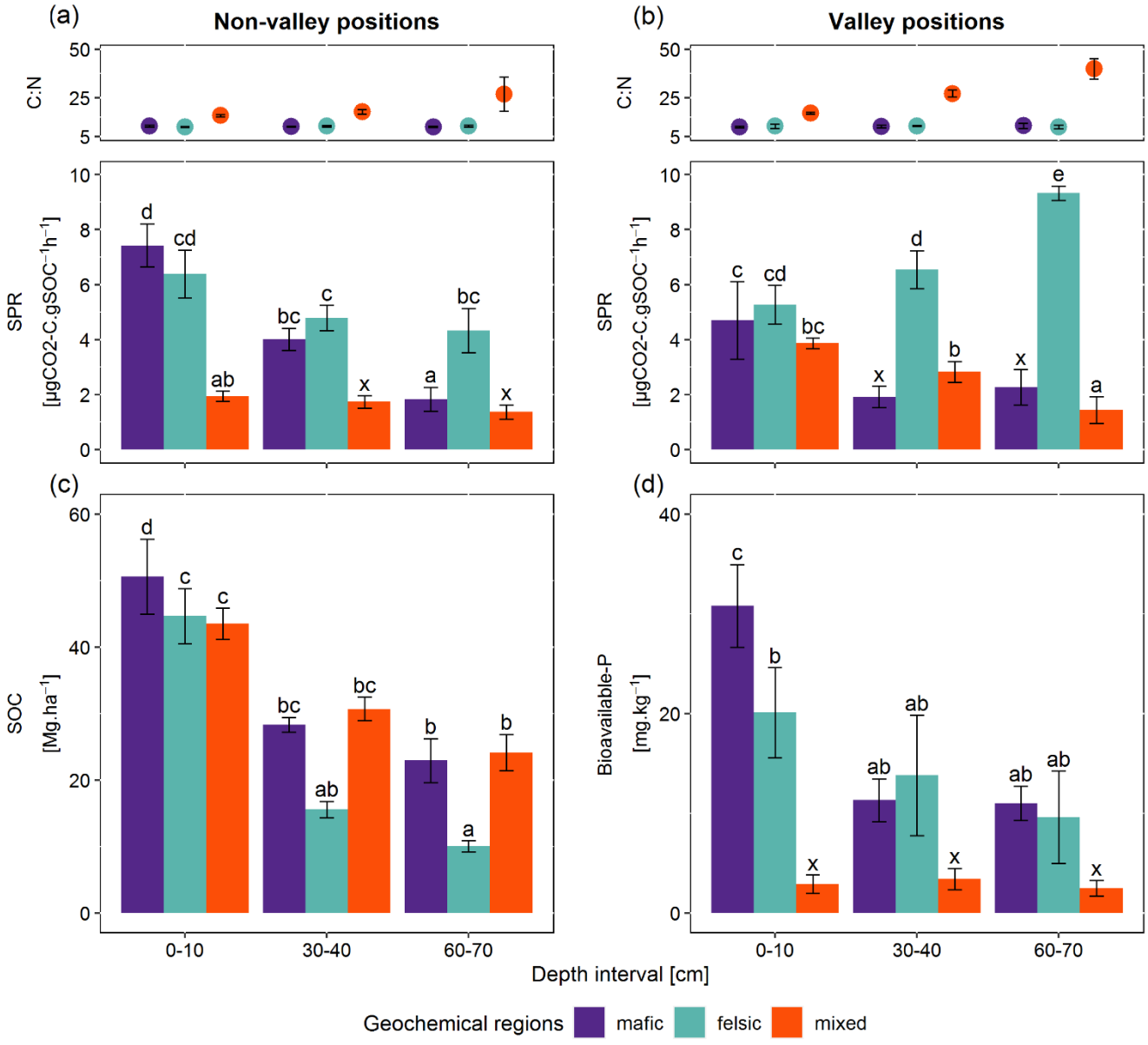

Figure 1. Average and standard errors based on field replicates, (**a**) C:N ratio as points (top) and specific potential respiration (SPR) bottom for non-valley positions (N = 9), (**b**) C:N ratio as points (top) and specific potential respiration (SPR) bottom for valley positions (n= 3), (**c**) SOC stocks and (**d**) Bioavailable phosphorus for non-valley positions (n = 9). Same letters on

top of bars indicate no significant difference following ANOVA tested for differences between geochemical regions and depth intervals. "x" indicates no significant difference between depth intervals within geochemical regions. ANOVA tests were performed separately for non-valley and valley positions.

3.2 Patterns and differences in $\Delta^{14}C$ of bulk soils vs. $\Delta^{14}C$ of respired CO_2

Across all study regions we found a strong relationship (R^2 = 0.81, $p<0.1$) between $\Delta^{14}C$ of the bulk soil and $\Delta^{14}C$ of the respired CO_2. In non-valley positions, soil C was consistently more depleted than its respired C counterparts, and depth trends in the $\Delta^{14}C$ of respired CO_2 were much less pronounced (Fig. 2a). Notably, the differences in $\Delta^{14}C$ between soil and CO_2 were consistently smaller in the felsic and mafic regions than in the mixed sediment region. In valley positions, differences in $\Delta^{14}C$ between soils and respired CO_2 generally followed the same trends as for non-valley positions, with the exception of the $\Delta^{14}C$ of respired CO_2 in the mixed sediment region being similarly depleted to the soil (Fig. 2a-b).

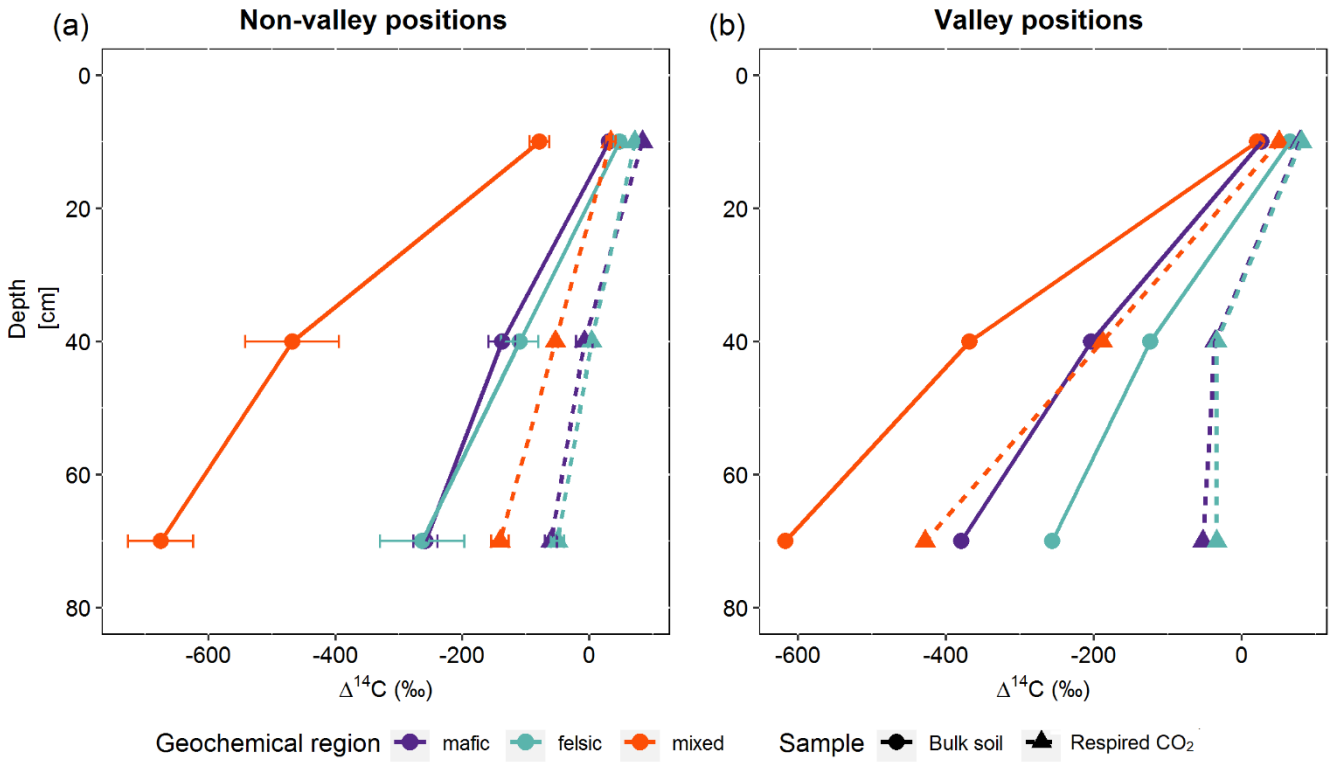

Figure 2: Average and standard errors based on all composite samples for non-valley positions only. (**a**) radiocarbon content ($\Delta^{14}C$) of the bulk soil and respired CO_2 for non-valley positions, (**b**) $\Delta^{14}C$ of the bulk soil and respired CO_2 for valley positions, (n = 27 for non-valleys, and n = 9 valleys for each depth interval). Note that at non-valley positions, each point in panel 2a

represents 3 observations from composite samples. At valley positions, each point in panel 2b represent 1 observation from composite samples.

We found a significant contribution of fossil organic C to both SOC and respired CO_2 in the mixed sediment region (Table 2). There, the calculated contribution of fossil organic C to total SOC in bulk soil and respired CO_2 increased with soil depth with similar trends for valley and non-valley positions. However, the calculated contribution of fossil organic C to respired CO_2 was much higher in valley subsoil (19-39% fossil organic C in respired CO_2) than in non-valley subsoil (7-9% fossil organic C in respired CO_2). Generally, the contribution of biogenic C to total C was consistently higher (61-97%) in respired CO_2 than in SOC of the corresponding bulk soil (48-98%) in both valley and non-valley positions. Microbial respiration discriminated against fossil organic C in non-valley positions by a factor of 3-7 (f_{FOC} bulk soil/respired CO_2), but did not discriminate against fossil organic C in valley positions (0.7-1.5 f_{FOC} bulk soil/respired CO_2).

Table 2. Biogenic and fossil organic carbon contribution in the mixed sediment region to SOC and respired CO_2 as % of total C and ratio bulk soil / respired C for both parameters. Values are displayed separately for non-valley and valley positions per soil depth (n = 1 per soil depth and position due to merging of replicates into composites prior to analysis). We note that these values are an upper bound on the contribution of fossil organic C, as these estimates may be affected by variable rates of biogenic C cycling.

		Biogenic [%]			Fossil [%]		
Position	Depth [cm]	Bulk soil	Respired gas	Bulk/Respired	Bulk soil	Respired gas	Bulk/Respired
Non-valley	0-10	89	96	0.9	11	4	2.8
	30-40	61	93	0.6	39	7	6.0
	60-70	48	91	0.5	52	9	5.8
Valley	0-10	98	97	1.0	2	3	0.7
	30-40	72	81	0.9	28	19	1.5
	60-70	57	61	0.9	43	39	1.1

3.3. Predicting SPR and Δ-$\Delta^{14}C$

Explanatory variables and mechanistic interpretation

For the non-valley subset of our data, rotated principal component analyses yielded 5 significant rotated components (RCs) that together explained 74.5% of the cumulative variance of the dataset (Table B1). From these components, RC1 and RC2 explained about 49% of the entire variance in the dataset, and were loaded with 13 (RC1) and 10 (RC2) independent but highly auto-correlated predictors within each RC. Predictors for RC1 related to soil organic matter characteristics and microbial activity. Predictors for RC2 related to the chemistry of the soil solution. RC3-RC5 explained about 5-11% of the variance

within the dataset with varying loading of 2-3 independent predictors that relate mechanistically to soil texture (RC3), aggregation (RC4) and C:N ratio + O horizon C stock (RC5).

Regressions and relative importance of RCs for predicting SPR and Δ-Δ^{14}C

Using the rotated components identified above and soil depth as an additional variable, SPR was predicted for the non-valley subset of our data with R^2 = 0.47 (RMSE = 1.9 µgCO_2-C gSOC^{-1}; n = 85). When predicting only topsoils, R^2 increased to 0.62 (RMSE = 1.7 µgCO_2-C gSOC^{-1}; n = 28). When predicting only subsoils, R^2 decreased to 0.32 (RMSE = 1.6 µgCO_2-C gSOC^{-1}; n = 57). Δ-Δ^{14}C was predicted similarly in all three submodels (R^2 = 0.75-0.94; RMSE = 18.1- 88.4 ‰) (Table 3). Besides soil depth, RC2 (soil solution chemistry) and RC3 (soil texture) were the most important predictors for SPR. Note that in subsoil, RC3 (soil texture) was no longer selected as a predictor for SPR although it was a highly important predictor in topsoil. Δ-Δ^{14}C, in general, was predicted by a wider range of variables than SPR. Topsoil Δ-Δ^{14}C was predicted by the RCs "soil solution chemistry", "C:N ratio" and "soil texture". In subsoil, Δ-Δ^{14}C was predicted by the RCs "SOM and microbial activity", "soil solution chemistry", "aggregation" as well as "C:N ratio and O horizon C stock". Note that RC4 "aggregation", related to the amount of C associated with microaggregates, played only a minor role as predictor in all data and subsoil predictions of Δ-Δ^{14}C. Aggregation did not contribute to the predictive power of topsoil Δ-Δ^{14}C and was not included in any model for predicting SPR.

Table 3. Results of three regression models (topsoil only, subsoil only, and all data) using RCs scores to predict SPR and Δ-Δ^{14}C including standardized coefficients and model performance indicators. For models using all data, soil depth was included as an additional explanatory variable. Blank cells indicate non-significant predictors (*p*-value<0.1) that were not selected by the model.

	Standardized Coefficients					
	Topsoil		Subsoil		All data	
Explanatory variables	SPR	Δ-Δ^{14}C	SPR	Δ-Δ^{14}C	SPR	Δ-Δ^{14}C
Soil depth					-0.3	-0.4
SOM and microbial activity (RC1)				0.4		0.2
Soil solution chemistry (RC2)	0.5	0.4	0.4	0.5	0.5	
Soil Texture (RC3)	-0.7	-0.4			-0.3	-0.1
Aggregation (RC4)				-0.3		-0.2
C:N ratio and O horizon (RC5)		-0.6		-0.5		-0.6
R^2	0.62	0.94	0.32	0.75	0.47	0.79
RMSE	1.7	18.1	1.6	87.4	1.9	88.4
F-stat	7.46	75.1	4.8	31.3	11.2	49.3
p-value	0.0001	<0.05	0.0056	<0.05	<0.05	<0.05

Controlling for soil depth (partial correlations)

Partial correlation analysis revealed little to no statistically significant changes in correlation between most RCs and our target variables when comparing zero-order and depth-controlled correlations (Fig. 3). However, a marked and significant reduction in correlation was observed between SPR and RC1 (SOM and microbial activity) as well as between Δ-$\Delta^{14}C$ and RC1 when controlling for soil depth. A smaller but significant reduction in correlation after introducing soil depth as a control was observed for SPR and RC4 (aggregation). Thus, the reduction in correlation after controlling for soil depth indicates that the relationship of those RC1 and RC4 to target variables is, in part, dependent on soil depth and cannot be interpreted fully independent.

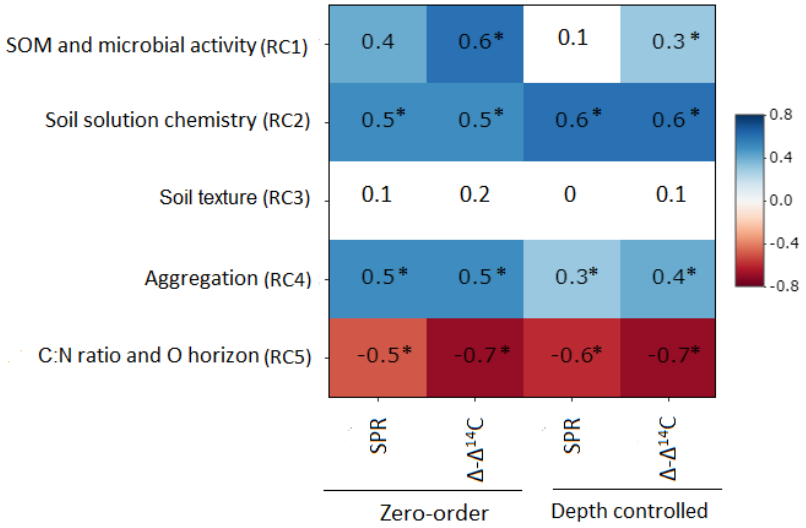

Figure 3. Zero order and partial correlation displayed as Pearson r between target variables (SPR and Δ-$\Delta^{14}C$) and explanatory variables, controlling for soil depth. Colour indicates the relationship (red = negative correlation, blue = positive correlation, white = weak correlation). The intensity of the colour indicates the strength of the correlation. Asterisks indicate that correlations are significant at *p*-value<0.1.

4. Discussion

Fertility and microbial activity

Across soil depth, the chemistry of the soil solution (RC2 composed of pH, base saturation, CEC, exchangeable acidity etc.) (Table B1) played an important role in predicting SPR and $\Delta^{14}C$ in our lab incubation experiment (Fig. 3, Table 3). Additionally, available nutrients (dissolved N and bioavailable P) reported by Kidinda et al. (2020) for the same soils as investigated, were positively correlated to SPR and $\Delta^{14}C$ of respired CO_2 (Fig. A1) in the mafic and felsic regions. Note that $\Delta^{14}C$ signatures of the bulk soil and respired CO_2 were nearly identical along depth intervals and between the two contrasting (mafic and felsic) parent materials (Fig. 2a). This suggests that the cycling of biogenic C, particularly in the topsoil, can act at a similar rate between soils developed from contrasting parent material (Fig. 3) if soil fertility constraints are satisfied. In contrast, in the mixed sediment region, poor soil fertility is likely one of the main causes of lower rates of C cycling in soil. Soils in this region had the lowest available nutrients, with substantially lower concentrations of bioavailable P (Fig.1d) and NH_4^+ (data not presented) than soils in the mafic and felsic regions. This adds to existing literature suggesting that nutrient limitation, especially N and P, can significantly inhibit microbial growth and activity, hence lowering soil C turnover rates (Fang et al., 2014; Kunito et al., 2009). In addition, the depletion of N and high C:N values (153.9 ± 68.5) of fossil organic C, which encompasses a substantial part of total C in subsoils of the mixed sediment region (Table 2), was likely an additional factor reducing soil respiration rates (Whitaker et al., 2014). However, respiration rates in the topsoil of the mixed sediment were also lower compared to the mafic or felsic region (Fig. 1), but fossil organic C content in the topsoil was low compared to the subsoil (Table 2). Thus, we conclude that for our investigated tropical forest systems, soil fertility constraints such as the composition of the soil solution (Table B2) are likely more important contributors to explain respiration rates than the presence of fossil organic C content or other C quality constraints.

The role of tropical weathering and mineral related C stabilization mechanisms in explaining soil respiration

In contrast to studies on soils in temperate climate zones (Franzluebbers and Arshad, 1997; Hassink, 1997; Schleuß et al., 2014), in our study aggregation and soil texture played only a secondary role in explaining variability in SPR and $\Delta^{14}C$, and their influence decreased with soil depth (Table 3). We explain this observation with the fact that clay minerals at advanced weathering stages such as kaolinite, dominating in tropical soils, generally show lower activity and reactive surfaces than clay minerals dominating earlier weathering stages (e.g. Smectite, Vermiculite) (Doetterl et al., 2018). Lower reactivity of these clays and reduced ability to complex with organic compounds reduce the capacity of the clay fraction to stabilize C in tropical soils compared to temperate soils (Six et al., 2002). In contrast, high amounts of Fe and Al (hydro-) oxides as a result of long term soil weathering have been shown to have a greater influence on C stabilization mechanisms and soil C content (von Fromm et al., 2021; Khomo et al., 2017; Reichenbach et al., 2021). For example, amorphous, oxalate extractable Fe or Al-oxides improve the stability of aggregates and can ultimately limit microbial activity (Kirsten et al., 2021; Nagy et al., 2018). Comparing our findings on SPR to the abundance of oxalate or DCB extractable Fe or Al amorphous and crystalline pedogenic

oxides reported by Reichenbach et al. (2021), we found weak to no correlation (Fig. A3 b-c). We interpret this result as an indication that C stabilized by such minerals does not contribute to soil respiration in a significant way in our short-term respiration experiment. Its effects on the long-term SOC stability are more likely related to the formation of stable aggregates (Kleber et al., 2005; Oades, 1988;Barthès et al., 2008; Rasmussen et al., 2018; Traoré et al., 2020; Quesada et al., 2020). Stable metal-organic complexes then represent energetic barriers in soil that are hard to overcome for microorganisms to access potential C resources (Bruun et al., 2010; Zech et al., 1997). The importance of these mechanisms is illustrated by the fact that although mafic soils were generally more fertile than soils in the felsic or mixed sediment region, SPR was lower and decreased more strongly with depth in mafic soils (75% decrease in deep subsoil compared to topsoil) than in felsic soils (33% decrease) (Fig. 1a). We argue that SOC stocks in the mafic region are higher and SPR lower due to the presence of mineral related stabilization mechanisms that are lacking in other regions, consistent with the findings of Reichenbach et al. (2021). Interestingly, our data suggests that C associated with pyrophosphate extractable oxides (organo-metallic complexes) is readily available to microbial decomposers and can contribute to respiration in a short-term experiment such as ours (Fig. A3a).

In summary, the contrasting relationship of pedogenic oxides of different origin and formation to SPR and $\Delta^{14}C$ illustrates the need to improve our understanding of metal-organic interactions and their role in C stabilization in tropical soils as our results seemingly confirm (role of metal oxides) and also contradict (role of clay) findings from younger soils in the temperate zone (Khomo et al., 2017). Our results, linked to those of Reichenbach et al. (2021), show that the presence or absence of mineral stabilization mechanisms is particularly important for long-term soil C stocks in tropical soils, varying largely with soil parent material, while short-term respiration relies on readily available C sources. However, given that annual plant C inputs are high in tropical forest systems (Lewis et al., 2009; Sayer et al., 2011), exceeding what deeply weathered soils can stabilize, the soil and environmental conditions under which C can be decomposed or stabilized seem to be more important for short-term respiration.

Accessibility of old C sources to microbial decomposers and its contribution to SOC

The presence of fossil organic C in the mixed sediment region (up to 52% of SOC stock in deeper subsoil) (Table 2), had a marked effect on SOC stocks in subsoils that would otherwise be similarly low to those of the felsic region (Fig. 1c). Consistent with this finding, a recent study shows that fossil organic C can largely contribute to SOC in subsoils (Kalks et al., 2021). While fossil organic C in our study region is of poor quality as indicated by depleted N and high C:N values (153.9 ± 68.5), our data shows that fossil organic C was microbially available (Fig. 2), leading to the respiration of CO_2 with comparably old ^{14}C signatures. However, we were unable to quantitatively disentangle the slower biogenic C cycling from the contribution of fossil organic C using $^{14}CO_2$. Thus, whether the presence of FOC and/or other unfavorable chemical soil characteristics in the mixed sediment region contributed to a general slowing of C cycling remains unknown.

Nevertheless, under the ideal conditions for microbial activity evoked by our experimental setup, similar to in situ topsoil conditions, microbial organisms can decompose these older, less accessible C sources thereby decreasing the residence time

of the fossil organic C (Hemingway et al., 2018). The fact that $\Delta^{14}C$ signatures in respired CO_2 do not mirror the signature of their C sources in soil indicates that microorganisms do continue to discriminate against these older, poorer C sources if alternatives are available (Fig. 2) (Feng et al., 2017).

Being a non-renewable source of organic matter, the fact that fossil organic C can still be found in topsoil is likely related on the one hand to the underlying erosion rates that continuously degrade the mountainous landscapes of the East African Rift System, and on the other hand to the discrimination against fossil organic C by microbial decomposers in the presence of other, more available C sources. While erosion rates at annual or decadal timescales are negligible for the investigated tropical forests (Drake et al., 2019; Wilken et al., 2021), underlying geological erosion rates estimated for tropical mountain forests globally (Morgan, 2005) range between 0.03-0.2 $t.ha^{-1}.y^{-1}$. Assuming an average bulk density in our study area's topsoil of roughly 1.3 $g.cm^{-3}$ (Doetterl et al., 2021), 6.8-45.3 k years are required to erode the top 10 cm of soil. Thus, slow erosion of soil at millennial timescales may explain the residual content of fossil organic C in topsoil. The loss of soil material as a result of slow processes of landscape denudation do not directly affect the biological processes investigated in our study. However, erosion at geological timescales cannot be ignored as a mechanism for the long-term rejuvenation of soil surfaces (Flores et al., 2020; Montgomery, 2007) in pristine tropical catchments, and, in our study, leading to the exposition of fossil C sources to surface conditions.

Respiration in tropical forests unaffected by lateral fluxes and only by in situ forest hydrological conditions

While we did not observe differences in respiration and $\Delta^{14}C$ along slope gradients within any of the geochemical regions, we observed significant differences in SPR between valley and non-valley positions (Fig. 1a-b). The absence of differences along slopes is a strong indicator that lateral fluxes of matter and water do not significantly influence SOC dynamics at timescales relevant to create topography dependent differences in C cycling. This finding is supported by work conducted at the global scale which found erosion in pristine tropical forests was negligible (Vågen and Winowiecki, 2019). Further, at the regional scale in our study region, Drake et al. (2019) found that riverine particulate matter draining from pristine tropical forest catchments are generally dominated by soluble and particulate organic matter fluxes, with little to no mineral sediment being transported. This result is a strong indicator for little to no erosion of mineral soil in pristine catchments, in agreement with our own findings.

In our study, the effect of topography was limited to differences in hydrological conditions between valleys and non-valley positions. At valley positions decomposition of C in subsoil was generally reduced due to the nearly continuous water saturation, limiting the supply of oxygen (Linn and Doran, 1984; Skopp et al., 1990). These conditions are likely present at our study sites as supported by our findings of extensive gleyic features in all studied subsoils in valley positions. However, under the ideal conditions for microbial decomposition of C during our laboratory experiment, decomposition of C from valley subsoil was often higher than at their non-valley counterparts (Fig. 1). We explain this observation with the presence of C

sources that, although sometimes have old $\Delta^{14}C$ signatures (Fig. 2), become readily available to decomposers once environmental constraints, such as water saturation, are removed (Fig. 1b).

5. Conclusions

Our study shows that geochemical differences in soils that are the result of soil formation from varying parent material (mafic, felsic and mixed sedimentary rocks) continue to influence the microbial activity, SOC stocks and C turnover in tropical soils even after many millennia of weathering and almost complete pedogenic alteration of the parent material. The chemistry of the soil solution, namely soil fertility, and the availability of P and N for microbial decomposers were identified as the most important variables explaining patterns of heterotrophic respiration under idealized well-aerated topsoil conditions. C stabilization mechanisms including the presence or absence of pedogenic oxides between our geochemical regions were identified as indirect controls to explain variation in soil respiration through their effect on soil aggregation and as potential energetic barriers that decomposers are forced to overcome. Patterns of $\Delta^{14}C$ with soil depth were largely driven by the presence or absence of fossil organic carbon of low quality, inherited from parent material. Under idealized well-aerated topsoil conditions, these fossil C sources became available to microbial decomposers, especially in the absence of better alternative energy and nutrient sources.

Furthermore, our analyses revealed that soil respiration was driven in parallel by contrasting processes, limiting microbial activity and slowing down C cycling. C in soil of the studied mixed sediment region was low in quality, resulting in low specific respiration, slower C cycling and high SOC stocks. C in soil of the mafic region was lower in accessibility due to its stabilization with minerals, also resulting in low specific respiration and high SOC stocks in subsoil. Thus, while geochemistry differed drastically between soils in those two systems, particularly in subsoils, both show low specific respiration for entirely different reasons. In contrast, soils in the felsic region showed high specific soil respiration, as no strong mineral driven stabilization mechanisms were present and as soil C of favorable quality was readily available for microorganisms to decompose.

While the impact of geochemistry on C dynamics was clearly distinct between the studied soils, topography only played a secondary role in these densely vegetated tropical forest systems. Hydrological features such as water saturation in valleys partially inhibited microbial activity in situ, leaving labile C sources available for decomposition under the idealized laboratory conditions of our experiment. Erosional processes rejuvenating soils and landscapes at geological timescales did account for significant differences in C cycling across geochemical regions due to the surfacing of fossil organic carbon, but did not act at timescales to create topography dependent differences in C cycling. We conclude from our findings that geochemistry, parent material and its lasting role on pedogenesis are key factors to consider to improve our understanding of C release from tropical forest soils. Improving the spatial representation of C dynamics at larger spatial scales using the variables and controls

identified in this study could potentially be an important improvement for predicting and modeling future C turnover in tropical forest soils.

6. Appendices

Appendix A-Figures

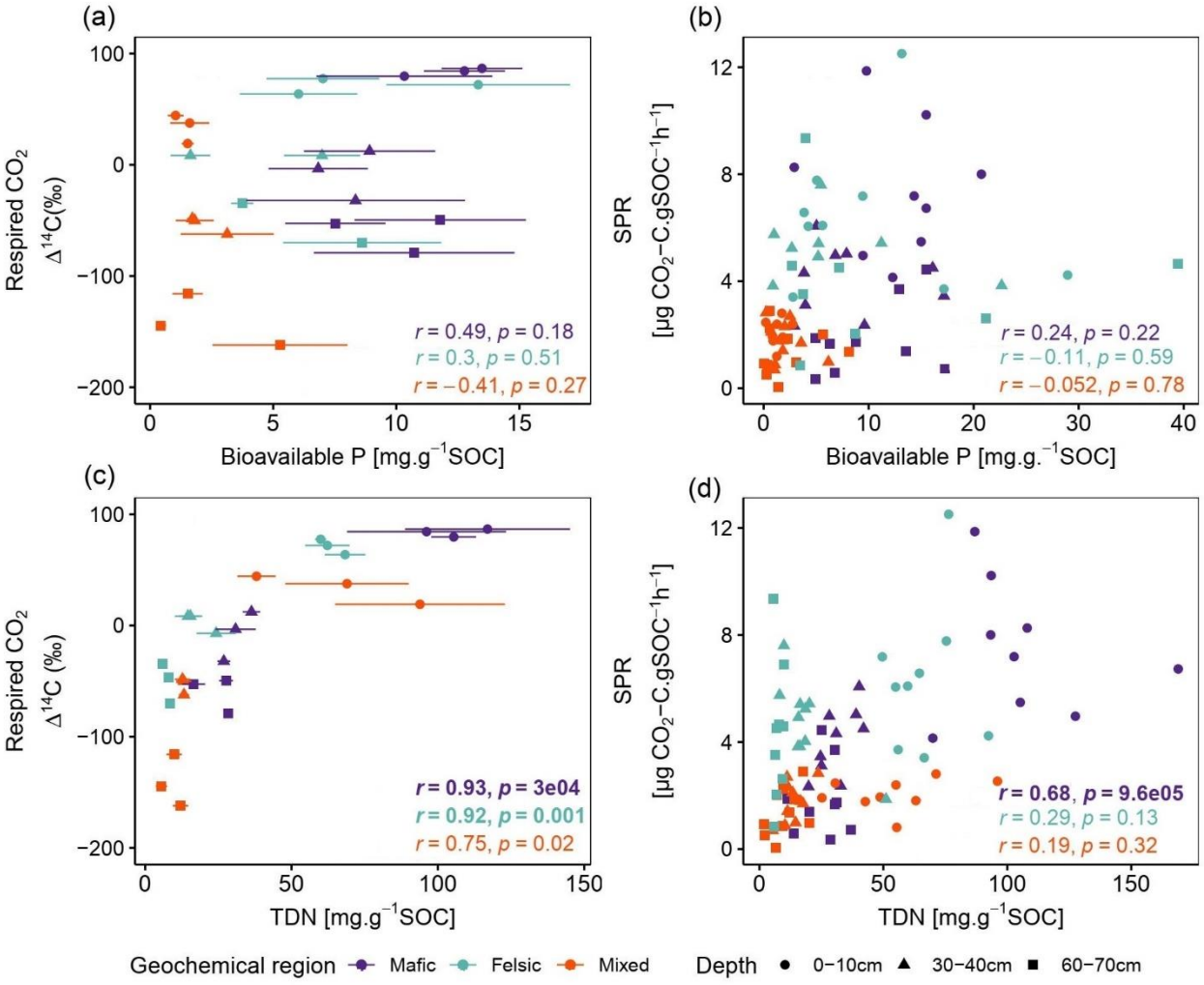

Figure A1. Pearson correlation between composite of corresponding replicates of $\Delta^{14}C$ of respired CO_2 and SPR to P (panels, a-b), and N (panels, c-d) available nutrient data reported by Kidinda et al.,(2020) normalized to SOC content for non-valley positions. Data displayed in panels a, and c, are averages plus standard errors of three field replicates. Panels b, and d, show all individual field replicates. Note that two outliers (artefacts) with high bioavailable P values in subsoil were removed from panels a, and b. p-values in bold font indicate significant results at $p<0.05$. Abbreviations: Bioavailable P = Bray-P, TDN = Total dissolved nitrogen.

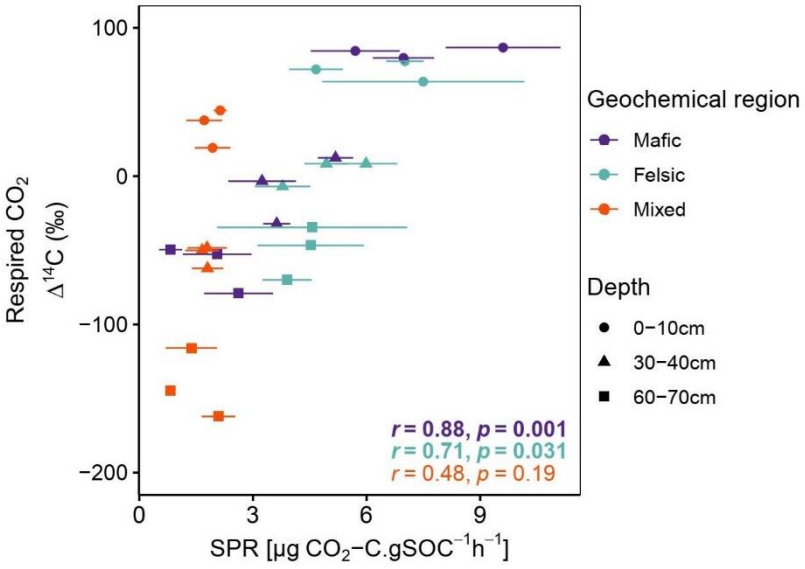

Figure A2. Pearson correlation between ^{14}C of respired CO_2 and SPR for non-valley positions. Data displayed are averages plus standard error of three field replicates (n = 85). p-values in bold font indicate significant results at p<0.05.

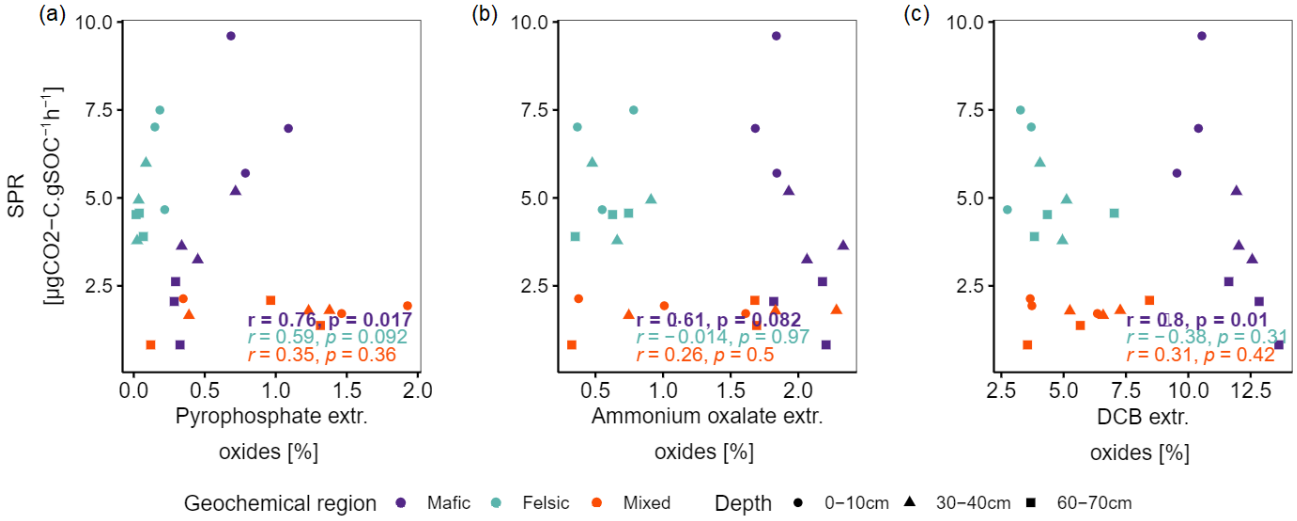

Figure A3. Pearson correlation between SPR and sum of pedogenic oxides (Al, Fe and Mn). panel (a) Sodium pyrophosphate extractable oxides, (b) ammonium oxalate-oxalic acid extractable oxides and (c) dithionite-citrate bicarbonate extractable oxides. p-values in bold font indicate significant results at p<0.05. Data reported by Reichenbach et al. (2021).

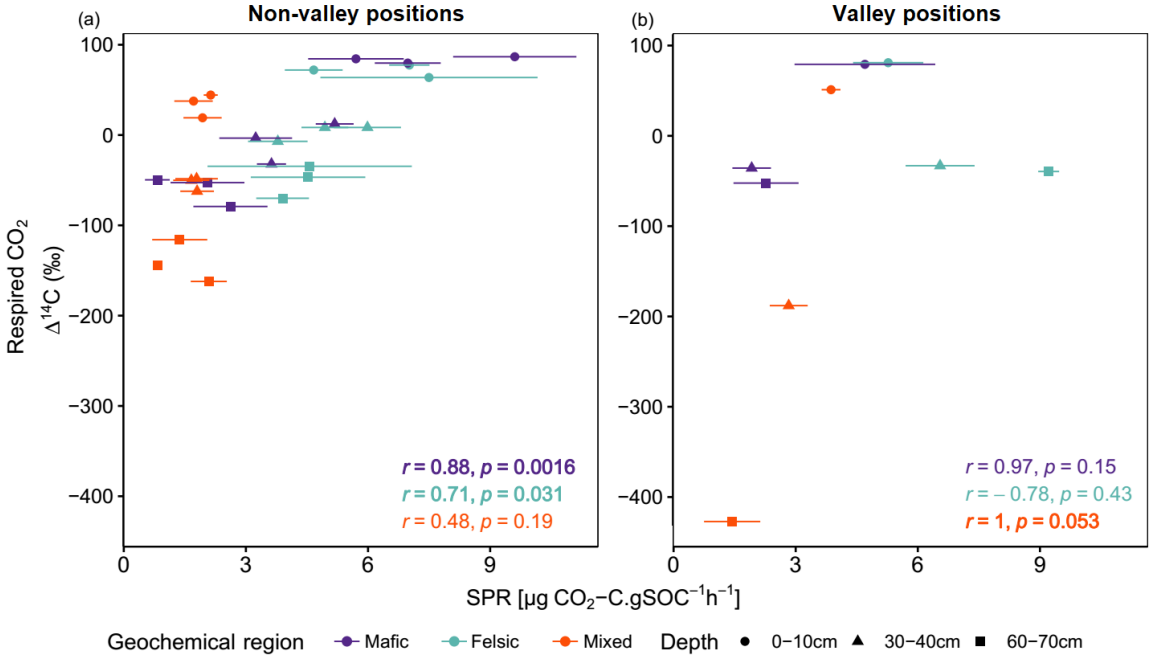

Figure A4. Pearson correlation between ^{14}C of respired CO_2 and SPR for (a) for non-valley positions and (b) for valley positions. Data displayed are averages plus standard error of three field replicates (non-valleys n = 85 and valley position n = 27). p-values in bold font indicate significant results at p<0.05.

Appendix B-Tables

Table B1. Rotated principal component analysis for six principal components (RC) retained with Eigenvalues >1 and proportion variance >5%. Upper part of the table shows eigenvalues, individual and cumulative variance and mechanistic interpretation of specific RCs. Bottom part represents loadings with bold marked and underlined values showing the highest loadings of each RC (r>0.5).

	Rotated component		RC1	RC2	RC3	RC4	RC5
	Eigenvalue		8.0	7.5	3.4	2.6	2.4
	Proportion variance (%)		25.0	23.6	10.5	8.0	7.5
	Cumulative variance (%)		25.0	48.6	59.1	67.1	74.5
	Mechanistic interpretation		SOM and microbial activity	Soil solution chemistry	Soil texture	Aggregation	C:N ratio and O horizon
	Independent variables	Units					
Microbial activity	Carbon enzymes	$nmol.g^{-1}.h^{-1}$	**0.6**	-0.1	-0.1	0.2	0.0
	Phosphorus enzymes	$nmol.g^{-1}.h^{-1}$	**0.7**	0.0	0.1	0.0	0.0
	Nitrogen enzymes	$nmol.g^{-1}.h^{-1}$	**0.6**	0.4	0.0	0.1	0.0
	Microbial biomass carbon	$mg.kg^{-1}$	**0.5**	0.3	-0.3	0.2	0.0
Nitrogen	Total dissolved nitrogen	$mg.kg^{-1}$	**0.9**	0.1	0.1	0.1	0.0
	Ammonium	$mg.kg^{-1}$	**0.9**	0.3	0.0	0.2	0.0
	Nitrate	$mg.kg^{-1}$	0.3	-0.1	0.2	0.0	0.0
	Nitrogen content	%	**1.0**	0.0	0.0	0.2	-0.1
Soil carbon	Dissolved organic carbon	$mg.kg^{-1}$	**0.8**	-0.3	-0.1	0.0	-0.1
	Carbon content	%	**0.9**	-0.2	0.1	0.1	0.0
	Soil organic carbon stock	$Mg.ha^{-1}$	**0.9**	-0.1	0.1	0.1	0.2
	C:N	-	-0.1	-0.1	0.0	-0.3	**0.8**
C fractions	Microaggregate/silt and clay	%	0.2	0.2	0.0	**0.9**	-0.1
	Relative amount of POM	%	0.0	0.1	**0.6**	0.1	0.2
	Relative amount of microaggregate	%	0.2	0.1	-0.3	**0.8**	-0.3
	Relative amount of silt and clay	%	-0.1	-0.1	-0.2	**-0.8**	0.1
Soil fertility	Exchangeable acidity	$me.100g^{-1}$	0.3	**-0.9**	0.0	0.0	0.0
	Exchangeable bases	$me.100g^{-1}$	0.3	**0.9**	0.1	0.1	-0.1
	Cations exchange capacity	$me.100g^{-1}$	**0.7**	-0.2	-0.4	0.2	-0.3
	Effective cations exchange capacity	$me.100g^{-1}$	**0.6**	**0.7**	0.1	0.1	-0.1
	Base saturation in ECEC	%	0.0	**0.9**	0.1	0.1	-0.3
	Base saturation in CEC	%	0.0	**1.0**	0.2	0.0	-0.1
	pH	-	-0.1	**0.9**	0.0	0.1	-0.1
	Plant available phosphorus	$mg.kg^{-1}$	**0.5**	**0.3**	0.0	-0.2	-0.3
Clay activity	pH:Clay	-	0.0	**0.5**	**0.8**	0.0	0.0
	Base saturation in ECEC/ Clay	-	0.0	**0.9**	0.3	0.1	-0.2
	Base saturation in CEC/clay	-	0.0	**0.9**	0.3	0.0	-0.1
Soil texture	Clay	%	-0.1	-0.2	**-0.9**	0.1	-0.2
	Silt	%	0.1	-0.3	-0.1	-0.1	**0.9**
	Sand	%	0.0	0.3	**0.9**	0.0	-0.3
C input	O horizon C stock	$Mg.ha^{-1}$	0.0	-0.5	0.2	-0.2	**0.6**

Table B2. Overview of soil properties and fertility indicators for the three geochemical regions and depth intervals. Abbreviations: $Base_{exc}$= sum of exchangeable bases, CEC = potential cation exchange capacity, ECEC = effective cation exchange capacity; pH_{KCl} =, bio-P = bioavailable phosphorus (Bray P method). Values reported are averages plus standard deviations (n = 85). Data reported by Doetterl et al. (2021a,b).

Geochemical region	Depth [cm]	$Base_{exc}$ [me.100g^{-1}]	CEC [me.100g^{-1}]	ECEC [me.100g^{-1}]	pH_{KCl}	TDN [mg.kg^{-1}]	Clay [%]	Silt [%]	Sand [%]
	0-10	17.2±3.6	19.3±3.4	18.1±3.8	5.33±0.59	141±21.7	35±4	10±2	54±5
Felsic	30-40	6.5±1.5	12.3±1.8	7.6±1.2	4.67±0.69	14.4±7.5	41±11	8±2	51±10
	60-70	5.1±2.2	11.2±2.5	6.5±1.5	4.44±0.72	3.8±1.3	49±9	7±3	44±8
	0-10	7.2±7.3	42.6±8.2	12.1±4.9	3.66±0.60	263.8±100.1	54±9	14±4	33±11
Mafic	30-40	2.6±2.7	32.6±2.8	7.6±1.3	3.6±0.33	44.7±13.9	66±7	14±4	20±4
	60-70	1.1±0.7	31.7±4.1	6.7±1	3.50±0.22	26.2±5.9	67±3	13±4	20±3
	0-10	0.3±0.1	23.1±9.6	8.3±1.5	3.01±0.20	140.8±87.5	36±12	20±9.	44±18
Mixed	30-40	0.2±0.1	14.8±5.5	4.9±0.9	3.57±0.16	20.1±6	49±14	19±8	32±14
	60-70	0.2±0.1	12.5±6.7	3.8±0.7	3.73±0.13	10.6±5.8	50±14	21±13	29±14

7. Data availability statement

All data used in this study is published in an open access project-specific database with a separate DOI https://doi.org/10.5880/fidgeo.2021.009. The specific data of this publication is available upon request from the corresponding author (S. Doetterl)

8. Sample availability

Remaining soil samples are logged and barcoded at the Department of Environmental Science at ETH Zurich, Switzerland. Where sample material is left, soil samples can be made available upon request through the corresponding authors (S. Doetterl).

9. Acknowledgements

This study was financed within DFG Emmy Noether group through "Tropical soil organic carbon dynamics along erosional disturbance gradients in relation to soil geochemistry and land use" (TROPSOC; project number 387472333). A.M.H. received funding from the European Research Council (ERC) under the European Union's Horizon 2020 research and innovation program (grant agreement No. 695101 (14Constraint)). The authors would like to thank collaborators of this project: International Institute of Tropical Agriculture (CGIAR-IITA), Max Planck Institute for Biogeochemistry, Institute of Soil Science and Site Ecology at Technical University Dresden, Sustainable Agroecosystems Group and the Soil Resources Group ETH Zurich and the Faculty of Agriculture at the Catholic University of Bukavu, Institut Congolais pour la Conservation de

la Nature (ICCN), Rwanda Development Board (RDB) and Uganda Wildlife Authority (UWA). The authors would also like to thank the whole TROPSOC team especially the student assistants for their important work in the laboratory and all field helpers who made the sampling campaign possible. A personal thanks to Sophie von Fromm for valuable feedback on the manuscript. Special thanks also to the editors of SOIL and the two reviewers who have guided the review process of this manuscript and gave many valuable comments that improved the manuscript.

10. Author contribution statement

S.D. led the hosting project. S.D., and P.F. designed the research. B.B. and L.K.K conducted the sampling campaign, B.B conducted lab experiments and analyzed the data. S.D., P.F., A.M.H. and B.B. interpreted the data. All authors contributed to the writing of the paper.

11. Competing interest

SD is a liaison editor of the special issue Tropical biogeochemistry of soils in the Congo Basin and the African Great Lakes region and PF is a topical editor of the SOIL journal. However, none of them were involved in the review process of this manuscript. All other authors declare that they have no conflict of interest.

12. Special issue statement

This article is part of the SOIL Special Issue: Tropical biogeochemistry of soils in the Congo Basin and the African Great Lakes region.

References

Angst, G., Messinger, J., Greiner, M., Häusler, W., Hertel, D., Kirfel, K., Kögel-Knabner, I., Leuschner, C., Rethemeyer, J. and Mueller, C. W.: Soil organic carbon stocks in topsoil and subsoil controlled by parent material, carbon input in the rhizosphere, and microbial-derived compounds, Soil Biol. Biochem., 122, 19–30, doi:10.1016/j.soilbio.2018.03.026, 2018.

Bauters, M., Drake, T. W., Verbeeck, H., Bodé, S., Hervé-Fernández, P., Zito, P., Podgorski, D. C., Boyemba, F., Makelele, I., Ntaboba, L. C., Spencer, R. G. M. and Boeckx, P.: High fire-derived nitrogen deposition on central African forests, Proc. Natl. Acad. Sci. U. S. A., 115, 549–554, doi:10.1073/pnas.1714597115, 2018.

Berhe, A. A., Harden, J. W., Torn, M. S. and Harte, J.: Linking soil organic matter dynamics and erosion-induced terrestrial carbon sequestration at different landform positions, J. Geophys. Res. Biogeosciences, 113, 1–12, doi:10.1029/2008JG000751, 2008.

Berhe, A. A., Harden, J. W., Torn, M. S., Kleber, M., Burton, S. D. and Harte, J.: Persistence of soil organic matter in eroding versus depositional landform positions, J. Geophys. Res. Biogeosciences, 117, 1–16, doi:10.1029/2011JG001790, 2012.

van Breugel, P., Kindt, R., Lillesø, J. P. B., Bingham, M., Demissew, S., Dudley, C., Friis, I., Gachathi, F., Kalema, J., Mbago,

F., Moshi, H. N., Mulumba, J., Namaganda, M., Ndangalasi, H. J., Ruffo, C. K., Védaste, M., Jamnadass, R. and Graudal, L.: Potential natural vegetation map of Eastern Africa (Burundi, Ethiopia, Kenya, Malawi, Rwanda, Tanzania, Uganda and Zambia):Version 2.0. [online] Available from: https://static-curis.ku.dk/portal/files/244367666/2_VECEA_Volume_11_Uganda.pdf, 2020.

Bruun, T., Elberling, B. and Christensen, B. T.: Soil Biology & Biochemistry Lability of soil organic carbon in tropical soils with different clay minerals, Soil Biol. Biochem., 42, 888–895, doi:10.1016/j.soilbio.2010.01.009, 2010.

Cerri, C., Feller, C., Balesdent, J., Victoria, R. and Plenecassagne, A.: Application du traçage isotopique en 13C, à l'étude de la dynamique de la matière organique dans les sols, Comptes Rendus l'Académie des Sci. Paris, t.300, série II, 300, 423–428, 1985.

Cleveland, C. C., Townsend, A. R., Taylor, P., Alvarez-Clare, S., Bustamante, M. M. C., Chuyong, G., Dobrowski, S. Z., Grierson, P., Harms, K. E., Houlton, B. Z., Marklein, A., Parton, W., Porder, S., Reed, S. C., Sierra, C. A., Silver, W. L., Tanner, E. V. J. and Wieder, W. R.: Relationships among net primary productivity, nutrients and climate in tropical rain forest: A pan-tropical analysis, Ecol. Lett., 14, 939–947, doi:10.1111/j.1461-0248.2011.01658.x, 2011.

Davidson, E. A. and Janssens, I. A.: Temperature sensitivity of soil carbon decomposition and feedbacks to climate change, Nature, 440, 165–173, doi:10.1038/nature04514, 2006.

Davidson, E. A., Trumbore, S. E. and Amundson, R.: Soil warming and organic carbon content, Nature, 408, 789–790, doi:10.1038/35048672, 2000.

Day, R. W. and Quinn, G. P.: Comparisons of treatments after an analysis of variance in ecology, Ecol. Monogr., 59, 433–463, doi:10.2307/1943075, 1989.

Doetterl, S., Kearsley, E., Bauters, M., Hufkens, K., Lisingo, J., Baert, G., Verbeeck, H. and Boeckx, P.: Aboveground vs. belowground carbon stocks in African tropical lowland rainforest: Drivers and implications, PLoS One, 10, 1–14, doi:10.1371/journal.pone.0143209, 2015a.

Doetterl, S., Stevens, A., Six, J., Merckx, R., Van Oost, K., Casanova Pinto, M., Casanova-Katny, A., Muñoz, C., Boudin, M., Zagal Venegas, E. and Boeckx, P.: Soil carbon storage controlled by interactions between geochemistry and climate, Nat. Geosci., 8(10), 780–783, doi:10.1038/ngeo2516, 2015b.

Doetterl, S., Berhe, A. A., Arnold, C., Bodé, S., Fiener, P., Finke, P., Fuchslueger, L., Griepentrog, M., Harden, J. W., Nadeu, E., Schnecker, J., Six, J., Trumbore, S., Van Oost, K., Vogel, C. and Boeckx, P.: Links among warming, carbon and microbial dynamics mediated by soil mineral weathering, Nat. Geosci., 11, 589–593, doi:10.1038/s41561-018-0168-7, 2018.

Doetterl, S., Asifiwe, R., Baert, G., Bamba, F., Bauters, M., Boeckx, P., Bukombe, B., Cadisch, G., Cooper, M., Cizungu, L., Hoyt, A., Kabaseke, C., Kalbitz, K., Kidinda, L., Maier, A., Mainka, M., Mayrock, J., Muhindo, D., Mujinya, B., Mukotanyi, S., Nabahungu, L., Reichenbach, M., Rewald, B., Six, J., Stegmann, A., Summerauer, L., Unseld, R., Vanlauwe, B., Van Oost, K., Verheyen, K., Vogel, C., Wilken, F. and Fiener, P.: Organic matter cycling along geochemical, geomorphic and disturbance gradients in forests and cropland of the African Tropics - Project TropSOC Database Version 1.0, Earth Syst. Sci. Data

Discuss., 2021, 1–46, doi:10.5194/essd-2021-73, 2021.

Drake, T. W., Van Oost, K., Barthel, M., Bauters, M., Hoyt, A. M., Podgorski, D. C., Six, J., Boeckx, P., Trumbore, S. E., Cizungu Ntaboba, L. and Spencer, R. G. M.: Mobilization of aged and biolabile soil carbon by tropical deforestation, Nat. Geosci., 12, 541–546, doi:10.1038/s41561-019-0384-9, 2019.

Fang, H., Wang, Y., Yu, G. and Minjie, X.: Changes in soil heterotrophic respiration , carbon availability , and microbial function in seven forests along a climate gradient, Ecol. Res., 29, 1077–1086, doi:10.1007/s11284-014-1194-6, 2014.

Fang, K., Qin, S., Chen, L., Zhang, Q. and Yang, Y.: Al/Fe Mineral Controls on Soil Organic Carbon Stock Across Tibetan Alpine Grasslands, J. Geophys. Res. Biogeosciences, 124, 247–259, doi:10.1029/2018JG004782, 2019.

Feng, W., Liang, J., Hale, L. E., Jung, C. G., Chen, J., Zhou, J., Xu, M., Yuan, M., Wu, L., Bracho, R., Pegoraro, E., Schuur, E. A. G. G., Luo, Y., Gyo, C., Ji, J., Zhou, J., Xu, M., Yuan, M., Wu, L., Bracho, R., Pegoraro, E., Schuur, E. A. G. G. and Luo, Y.: Enhanced decomposition of stable soil organic carbon and microbial catabolic potentials by long-term field warming, Glob. Chang. Biol., 23(October 2016), 11, doi:10.1111/gcb.13755, 2017.

Fernández-Martínez, M., Vicca, S., Janssens, I. A., Sardans, J., Luyssaert, S., Campioli, M., Chapin Iii, F. S., Ciais, P., Malhi, Y., Obersteiner, M., Papale, D., Piao, S. L., Reichstein, M., Rodà, F. and Peñuelas, J.: Nutrient availability as the key regulator of global forest carbon balance, Nat. Clim. Chang. |, 4, doi:10.1038/NCLIMATE2177, 2014.

Fick, S. E. and Hijmans, R. J.: WorldClim 2: new 1-km spatial resolution climate surfaces for global land areas, Int. J. Climatol., 37, 12, doi:10.1002/joc.5086, 2017.

Fisher, J. B., Malhi, Y., Torres, I. C., Metcalfe, D. B., van de Weg, M. J., Meir, P., Silva-Espejo, J. E. and Huasco, W. H.: Nutrient limitation in rainforests and cloud forests along a 3,000-m elevation gradient in the Peruvian Andes, Oecologia, 172, 889–902, doi:10.1007/s00442-012-2522-6, 2013.

Flores, B. M., Staal, A., Jakovac, C. C., Hirota, M., Holmgren, M. and Oliveira, R. S.: Soil erosion as a resilience drain in disturbed tropical forests, Plant Soil, 450, 11–25, doi:10.1007/s11104-019-04097-8, 2020.

Fontaine, S., Barot, S., Barré, P., Bdioui, N., Mary, B. and Rumpel, C.: Stability of organic carbon in deep soil layers controlled by fresh carbon supply, Nature, 450, 277–280, doi:10.1038/nature06275, 2007.

Franzluebbers, A. J. and Arshad, M. A.: Particulate Organic Carbon Content and Potential Mineralization as Affected by Tillage and Texture, Soil Sci. Soc. Am. J., 61, 1382–1386, doi:10.2136/sssaj1997.03615995006100050014x, 1997.

von Fromm, S. F., Hoyt, A. M., Lange, M., Acquah, G. E., Aynekulu, E., Berhe, A. A., Haefele, S. M., McGrath, S. P., Shepherd, K. D., Sila, A. M., Six, J., Towett, E. K., Trumbore, S. E., Vågen, T.-G., Weullow, E., Winowiecki, L. A. and Doetterl, S.: Continental-scale controls on soil organic carbon across sub-Saharan Africa, SOIL, 7(1), 305–332, doi:10.5194/soil-7-305-2021, 2021.

Haaf, D., Six, J. and Doetterl, S.: Global patterns of geo-ecological controls on the response of soil respiration to warming, Nat. Clim. Chang., 11(7), 623–627, doi:10.1038/s41558-021-01068-9, 2021.

Hassink, J.: The capacity of soils to preserve organic C and N by their association with clay and silt particles, Plant Soil, 191,

77–87, doi:10.1023/A:1004213929699, 1997.

Hemingway, J. D., Hilton, R. G., Hovius, N., Eglinton, T. I., Haghipour, N., Wacker, L., Chen, M. C. and Galy, V. V.: Microbial oxidation of lithospheric organic carbon in rapidly eroding tropical mountain soils, Science (80-.)., 360, 209–212, doi:10.1126/science.aao6463, 2018.

IUSS Working Group WRB: World reference base for soil resources. International soil classification system for naming soils and creating legends for soil maps, Rome. [online] Available from: http://www.fao.org/3/i3794en/I3794en.pdf, 2015.

James, G., Witten, D., Hastie, T. and Tibishirani, R.: An Introduction to Statistical Learning with Applications in R (older version), Springer New York, New York, USA., 2013.

Jing, X., Chen, X., Fang, J., Ji, C., Shen, H., Zheng, C. and Zhu, B.: Soil microbial carbon and nutrient constraints are driven more by climate and soil physicochemical properties than by nutrient addition in forest ecosystems, Soil Biol. Biochem., 141, 107657, doi:10.1016/j.soilbio.2019.107657, 2020.

Jolliffe, I. T.: Rotation of principal components : choice of normalization constraints Rotation of principal components : choice of normalization constraints, J. Appl. Stat., 22, 29–35, doi:10.1080/757584395, 1995.

Kalks, F., Noren, G., Mueller, C. W., Helfrich, M., Rethemeyer, J. and Don, A.: Geogenic organic carbon in terrestrial sediments and its contribution to total soil carbon, SOIL, 7(2), 347–362, doi:10.5194/soil-7-347-2021, 2021.

Kearsley, E., De Haulleville, T., Hufkens, K., Kidimbu, A., Toirambe, B., Baert, G., Huygens, D., Kebede, Y., Defourny, P., Bogaert, J., Beeckman, H., Steppe, K., Boeckx, P. and Verbeeck, H.: Conventional tree height-diameter relationships significantly overestimate aboveground carbon stocks in the Central Congo Basin, Nat. Commun., 4, 8, doi:10.1038/ncomms3269, 2013.

Khomo, L., Trumbore, S. E., Bern, C. R. and Chadwick, O. A.: Timescales of carbon turnover in soils with mixed crystalline mineralogies, SOIL, 3, 17–30, doi:10.5194/soil-3-17-2017, 2017.

Kidinda, L. K., Olagoke, F. K., Vogel, C., Kalbitz, K. and Doetterl, S.: Patterns of microbial processes shaped by parent material and soil depth in tropical rainforest soils, SOIL Discuss., (December), 1–25, doi:https://doi.org/10.5194/soil-2020-80, 2020.

Kirsten, M., Mikutta, R., Vogel, C., Thompson, A., Mueller, C. W., Kimaro, D. N., Bergsma, H. L. T., Feger, K. H. and Kalbitz, K.: Iron oxides and aluminous clays selectively control soil carbon storage and stability in the humid tropics, Sci. Rep., 11(1), 1–12, doi:10.1038/s41598-021-84777-7, 2021.

Köchy, M., Hiederer, R. and Freibauer, A.: Global distribution of soil organic carbon – Part 1: Masses and frequency distributions of SOC stocks for the tropics, permafrost regions, wetlands, and the world, Soil, 1, 351–365, doi:10.5194/soil-1-351-2015, 2015.

Kramer, M. G. and Chadwick, O. A.: Climate-driven thresholds in reactive mineral retention of soil carbon at the global scale, Nat. Clim. Chang., 8, 1104–1108, doi:10.1038/s41558-018-0341-4, 2018.

Kunito, T., Akagi, Y., Park, H. D. and Toda, H.: Influences of nitrogen and phosphorus addition on polyphenol oxidase activity

in a forested Andisol, Eur. J. For. Res., 128, 361–366, doi:10.1007/s10342-009-0271-9, 2009.

Kwon, H. Y., Mueller, S., Dunn, J. B. and Wander, M. M.: Modeling state-level soil carbon emission factors under various scenarios for direct land use change associated with United States biofuel feedstock production, Biomass and Bioenergy, 55, 299–310, doi:10.1016/j.biombioe.2013.02.021, 2013.

Lewis, S. L., Lopez-Gonzalez, G., Sonké, B., Affum-Baffoe, K., Baker, T. R., Ojo, L. O., Phillips, O. L., Reitsma, J. M., White, L., Comiskey, J. A., Djuikouo K, M. N., Ewango, C. E. N., Feldpausch, T. R., Hamilton, A. C., Gloor, M., Hart, T., Hladik, A., Lloyd, J., Lovett, J. C., Makana, J. R., Malhi, Y., Mbago, F. M., Ndangalasi, H. J., Peacock, J., Peh, K. S. H., Sheil, D., Sunderland, T., Swaine, M. D., Taplin, J., Taylor, D., Thomas, S. C., Votere, R. and Wöll, H.: Increasing carbon storage in intact African tropical forests, Nature, 457, 1003–1006, doi:10.1038/nature07771, 2009.

Linn, D. M. and Doran, J. W.: Effect of Water-Filled Pore Space on Carbon Dioxide and Nitrous Oxide Production in Tilled and Nontilled Soils, Soil Sci. Soc. Am. J., 48, 1267–1272, doi:https://doi.org/10.2136/sssaj1984.03615995004800060013x, 1984.

Liu, L., Gundersen, P., Zhang, W., Zhang, T., Chen, H. and Mo, J.: Effects of nitrogen and phosphorus additions on soil microbial biomass and community structure in two reforested tropical forests, Sci. Rep., 5, doi:10.1038/srep14378, 2015.

Luo, Z., Feng, W., Luo, Y., Baldock, J. and Wang, E.: Soil organic carbon dynamics jointly controlled by climate, carbon inputs, soil properties and soil carbon fractions, Glob. Chang. Biol., 23, 4430–4439, doi:10.1111/gcb.13767, 2017.

Luo, Z., Wang, G. and Wang, E.: Global subsoil organic carbon turnover times dominantly controlled by soil properties rather than climate, Nat. Commun., 10, 1–10, doi:10.1038/s41467-019-11597-9, 2019.

Montgomery, D. R.: Soil erosion and agricultural sustainability, in Proceedings of the National Academy of Sciences of the United States of America, vol. 104, pp. 13268–13272., 2007.

Morgan, R. P. C.: Soil erosion & Conservation, 3rd ed., Blackwell Science Ltd, Massachusetts, USA., 2005.

Nagy, R. C., Porder, S., Brando, P., Davidson, E. A., Figueira, A. M. e. S., Neill, C., Riskin, S. and Trumbore, S.: Soil Carbon Dynamics in Soybean Cropland and Forests in Mato Grosso, Brazil, J. Geophys. Res. Biogeosciences, 123(1), 18–31, doi:10.1002/2017JG004269, 2018.

Ngongo, M. ., Van Ranst, E., Baert, G., Kasongo, E. L., Verdoodt, A., Mujinya, B. B. and Mukalay, J. .: Guide des Sols en R.D. Congo. Tome 1 : Etude et Gestion, 1st ed., Ecole Technique Salama-Don Bosco., 2009.

Quesada, C. A., Paz, C., Oblitas Mendoza, E., Phillips, O. L., Saiz, G., Lloyd, J., Alberto Quesada, C., Paz, C., Oblitas Mendoza, E., Lawrence Phillips, O., Saiz, G. and Lloyd, J.: Variations in soil chemical and physical properties explain basin-wide Amazon forest soil carbon concentrations, SOIL, 6(1), 53–88, doi:10.5194/soil-6-53-2020, 2020.

R Core Team: R: A language and environment for statistical computing., R Found. Stat. Comput., 2019.

Raich, J. W. and Schlesinger, W. H.: The global carbon dioxide flux in soil respiration and its relationship to vegetation and climate, Tellus B, 44, 81–99, doi:10.1034/j.1600-0889.1992.t01-1-00001.x, 1992.

Rasmussen, C., Heckman, K., Wieder, W. R., Keiluweit, M., Lawrence, C. R., Berhe, A. A., Blankinship, J. C., Crow, S. E.,

Druhan, J. L., Hicks Pries, C. E., Marin-Spiotta, E., Plante, A. F., Schädel, C., Schimel, J. P., Sierra, C. A., Thompson, A. and Wagai, R.: Beyond clay: towards an improved set of variables for predicting soil organic matter content, Biogeochemistry, 137, 297–306, doi:10.1007/s10533-018-0424-3, 2018.

Reichenbach, M., Fiener, P., Garland, G., Griepentrog, M., Six, J. and Doetterl, S.: The role of geochemistry in organic carbon stabilization in tropical rainforest soils, Soil, 1–35, doi:10.5194/soil-2020-92, 2021.

Rey, A., Petsikos, C., Jarvis, P. G. and Grace, J.: Effect of temperature and moisture on rates of carbon mineralization in a Mediterranean oak forest soil under controlled and field conditions, Eur. J. Soil Sci., 56(5), 589–599, doi:10.1111/j.1365-2389.2004.00699.x, 2005.

Sayer, E. J., Heard, M. S., Grant, H. K., Marthews, T. R. and Tanner, E. V. J.: Soil carbon release enhanced by increased tropical forest litterfall, Nat. Clim. Chang., 1(6), 304–307, doi:10.1038/nclimate1190, 2011.

Schimel, D. and Braswell, B. H.: The Role of Mid-latitude Mountains in the Carbon Cycle: Global Perspective and a Western US Case Study, in Global Perspective and a Western US Case Study, pp. 449–456., 2005.

Schimel, D., Stephens, B. B. and Fisher, J. B.: Effect of increasing CO2 on the terrestrial carbon cycle, Proc. Natl. Acad. Sci. U. S. A., doi:10.1073/pnas.1407302112, 2015.

Schleuß, P. M., Heitkamp, F., Leuschner, C., Fender, A. C. and Jungkunst, H. F.: Higher subsoil carbon storage in species-rich than species-poor temperate forests, Environ. Res. Lett., 9, 11, doi:10.1088/1748-9326/9/1/014007, 2014.

Schlüter, T.: Geological Atlas of Africa: with Notes on Stratigraphy, Tectonics, Economic Geology, Geohazard and Geosites of Each Country, Springer, Berlin,., 2006.

Schuur, E. A. G., Trumbore, S. E. and Druffel, E. R. M.: Radiocarbon and Climate Change: Mechanisms, Applications and Laboratory Techniques, Springer International Publishing., 2016.

Shapiro, S. S. and Wilk, M. B.: An Analysis of Variance Test for Normality (Complete Samples), Biometrika, 52, 591–611, doi:10.2307/2333709, 1965.

Shi, Z., Allison, S. D., He, Y., Levine, P. A., Hoyt, A. M., Beem-Miller, J., Zhu, Q., Wieder, W. R., Trumbore, S. and Randerson, J. T.: The age distribution of global soil carbon inferred from radiocarbon measurements, Nat. Geosci., 13, 555–559, doi:10.1038/s41561-020-0596-z, 2020.

Sierra, C. A., Hoyt, A. M., He, Y. and Trumbore, S. E.: Soil Organic Matter Persistence as a Stochastic Process: Age and Transit Time Distributions of Carbon in Soils, Global Biogeochem. Cycles, 32(10), 1574–1588, doi:10.1029/2018GB005950, 2018.

Six, J., Conant, R. T., Paul, E. A. and Paustian, K.: Stabilization mechanisms of soil organic matter: Implications for C-saturation of soils, Plant Soil, 241, 155–176, doi:10.1023/A:1016125726789, 2002.

Skopp, J., Jawson, M. D. and Doran, J. W.: Steady-State Aerobic Microbial Activity as a Function of Soil Water Content, Soil Sci. Soc. Am. J., 54, 1619–1625, doi:https://doi.org/10.2136/sssaj1990.03615995005400060018x, 1990.

Steinhof, A., Altenburg, M. and Machts, H.: Sample Preparation at the Jena 14C Laboratory, Radiocarbon, 59, 3,

doi:10.1017/RDC.2017.50, 2017.

Stuiver, M. and Polach, H. A.: Discussion Reporting of 14 C Data, Radiocarbon, 19, 9, doi:10.1017/s0033822200003672, 1977.

Tamhane, A. C.: A Comparison of Procedures for Multiple Comparisons of Means with Unequal Variances, J. Am. Stat. Assoc., 74, 471–480, doi:10.2307/2286358, 1979.

Torres-Sallan, G., Schulte, R. P. O., Lanigan, G. J., Byrne, K. A., Reidy, B., Simó, I., Six, J. and Creamer, R. E.: Clay illuviation provides a long-term sink for C sequestration in subsoils, Sci. Rep., 7(1), 45635, doi:10.1038/srep45635, 2017.

Trumbore, S.: Radiocarbon and soil carbon dynamics, Annu. Rev. Earth Planet. Sci., 37, 47–66, doi:10.1146/annurev.earth.36.031207.124300, 2009.

Tyukavina, A., Stehman, S. V., Potapov, P. V., Turubanova, S. A., Baccini, A., Goetz, S. J., Laporte, N. T., Houghton, R. A. and Hansen, M. C.: National-scale estimation of gross forest aboveground carbon loss: A case study of the Democratic Republic of the Congo, Environ. Res. Lett., 8, 14, doi:10.1088/1748-9326/8/4/044039, 2013.

Vågen, T. G. and Winowiecki, L. A.: Predicting the spatial distribution and severity of soil erosion in the global tropics using satellite remote sensing, Remote Sens., 11, 1–18, doi:10.3390/rs11151800, 2019.

Verhegghen, A., Mayaux, P., De Wasseige, C. and Defourny, P.: Mapping Congo Basin vegetation types from 300 m and 1 km multi-sensor time series for carbon stocks and forest areas estimation, Biogeosciences, 9, 5061–5079, doi:10.5194/bg-9-5061-2012, 2012.

Vitousek, P. M. and Chadwick, O. A.: Pedogenic Thresholds and Soil Process Domains in Basalt-Derived Soils, Ecosystems, 16, 1379–1395, doi:10.1007/s10021-013-9690-z, 2013.

Wilken, F., Fiener, P., Ketterer, M., Meusburger, K., Muhindo, D. I., van Oost, K. and Doetterl, S.: Assessing soil redistribution of forest and cropland sites in wet tropical Africa using 239+240Pu fallout radionuclides, SOIL, 7(2), 399–414, doi:10.5194/soil-7-399-2021, 2021.

Wright, S. J., Yavitt, J. B., Wurzburger, N., Turner, B. I., Tanner, E. V. J., Sayer, E. J., Santiago, L. S., Kaspari, M., Hedin, L. O., Harms, K. E., Garcia, M. N. and Corre, M. D.: Potassium, phosphorus, or nitrogen limit root allocation, tree growth, or litter production in a lowland tropical forest, Ecology, 92, 1616–1625, doi:10.1890/10-1558.1, 2011.

Xu, L., Saatchi, S. S., Shapiro, A., Meyer, V., Ferraz, A., Yang, Y., Bastin, J. F., Banks, N., Boeckx, P., Verbeeck, H., Lewis, S. L., Muanza, E. T., Bongwele, E., Kayembe, F., Mbenza, D., Kalau, L., Mukendi, F., Ilunga, F. and Ebuta, D.: Spatial Distribution of Carbon Stored in Forests of the Democratic Republic of Congo, Sci. Rep., 7, 1–12, doi:10.1038/s41598-017-15050-z, 2017.

Zech, W., Senesi, N., Guggenberger, G., Kaiser, K., Miano, T. M., Miltner, A. and Schroth, G.: Factors controlling humification and mineralization of soil organic matter in the tropics, Geoderma, 79, 117–161, doi:https://doi.org/10.1016/S0016-7061(97)00040-2, 1997.